

https://doi.org/10.1070/QEL17182

Quantum dot polarisation converter in an optomechanical cavity

A.V. Tsukanov, I.Yu. Kateev

Abstract. **We propose a scheme of a quantum photon polarisation converter, which is based on controlled electron–photon–phonon transitions in a hybrid semiconductor nanostructure. This structure consists of a GaAs/InAs quantum dot (QD) that has a parallelepiped shape and contains a single electron, and an optomechanical microcavity (MC) based on a photonic crystal (PC) that supports two orthogonally polarised photonic modes and one mechanical (phonon) mode. Within the framework of the microscopic theory, the QD and MC performance characteristics are found. Populations of states of the system as functions of time and its parameters are calculated. The principal possibility of photon polarisation conversion using transitions in a five-level resonance scheme for coherent (single-photon) and steady-state (subphoton) regimes is shown. The MC optical and mechanical spectra are simulated, and the PC structure parameters are selected to ensure the efficient operation of the converter.**

Keywords: *quantum dot, microcavity, polarisation, photonic crystal, optical phonons, optomechanics.*

1. Introduction

The development of technology for manufacturing nanostructures with a characteristic size of less than 1 μm has led to the emergence of new areas of experimental quantum physics. They include solid-state quantum optics, which studies, in particular, the interaction of discrete-spectrum nano-objects with external fields [1]. Many phenomena of traditional quantum optics, which deals with 'natural' atoms and molecules, are also observed in 'artificial' atoms, such as semiconductor quantum dots (QDs) [2], superconducting cavities, quantum bits (qubits) [3], and crystal lattice defects [4]. By 2010, the concept of a quantum chip, i.e. a device that combines the main functional elements for encoding, processing and transmitting quantum information, had been formulated and partially implemented [5]. The dynamics of processes in a chip is controlled by quantum fields: single photons are used as transport qubits, and subphoton pulses are used to measure the states of individual chip elements.

The choice of electromagnetic radiation polarisation is of great importance in the development of optical control circuits. It is especially important to be able to control the polarisation vector of the field interacting with high-spatial-symmetry systems, which are characterised by the pronounced selection rules for internal transitions. In this regard, it is necessary to be able to form fields with specified orthogonal components, as well as convert one component to another. Usually, the polarisation of a macroscopic laser beam is changed using a phase shifter (a plate placed in the path of beam propagation) [6]. However, for single photons propagating through a single-mode optical fibre from one qubit to another, this option may not be acceptable due to the absorption of photons by the plate material. Therefore, a different approach to the development of this circuit node is required. There are proposals for using the quantum nonlinearity effect in an optical cavity with a QD, which allows for small phase rotations of the photon polarisation vector in the regime of large detuning of the photon frequency from the QD frequency [7].

In our work, we propose a device that converts a single polarised photon into an orthogonally polarised photon due to its coherent interaction with a single-electron QD and a phonon mode. In this case, frequency conversion is also possible, which assumes scattering the excess photon energy into the phonon reservoir. The same is true for laser fields with low (subphoton) intensity, which are used in transmission spectroscopy and reflectometry [8]. In this case, the light passing through the system will be polarised orthogonally to the incident light. A semiconductor QD is placed in a microcavity (MC) based on a photonic crystal (PC) that supports two photonic modes with orthogonal polarisations and one mechanical mode. Within the framework of the microscopic theory, the QD and MC performance characteristics were found, and the populations of states of the system as functions of time and its parameters were calculated. The principal possibility of photon polarisation conversion using transitions in a five-level resonance scheme for coherent (single-photon) and steady-state (subphoton) regimes is shown.

2. Quantum hybrid converter model

We consider a single QD in the form of a parallelepiped with the characteristic sizes L_x, L_y and L_z along the corresponding Cartesian axes. We assume that the QD is located in a thin semiconductor plate which represents a mechanical cavity (Fig. 1). The low-lying electronic states of such a QD correspond with good accuracy to the model of a three-dimensional quantum well with infinitely high walls. Its energy spectrum has the form

$$\mathcal{E}(n_1, n_2, n_3) = \frac{\hbar^2\pi^2 n_1^2}{2m^* L_x^2} + \frac{\hbar^2\pi^2 n_2^2}{2m^* L_y^2} + \frac{\hbar^2\pi^2 n_3^2}{2m^* L_z^2},$$

A.V. Tsukanov, I.Yu. Kateev Valiev Institute of Physics and Technology, Russian Academy of Sciences, Nakhimovskii prosp. 34, 117218 Moscow, Russia, e-mail: ikateyev@mail.ru

Received 7 November 2019
Kvantovaya Elektronika **50** (3) 291–298 (2020)
Translated by M.A. Monastyrskiy

$$n_k = 1, 2, 3, ..., \quad (1)$$

where m^* is the effective mass of the electron. Hereafter, we restrict ourselves to three QD states: the ground state (g) and two almost degenerate excited (x and y) states with spatial wave functions.

$$\psi_g(\boldsymbol{r}) = \sqrt{\frac{8}{L_x L_y L_z}} \cos\left(\frac{\pi x}{L_x}\right)\cos\left(\frac{\pi y}{L_y}\right)\cos\left(\frac{\pi z}{L_z}\right),$$

$$n_1 = n_2 = n_3 = 1,$$

$$\psi_x(\boldsymbol{r}) = \sqrt{\frac{8}{L_x L_y L_z}} \sin\left(\frac{2\pi x}{L_x}\right)\cos\left(\frac{\pi y}{L_y}\right)\cos\left(\frac{\pi z}{L_z}\right), \quad (2)$$

$$n_1 = 2,\ n_2 = n_3 = 1,$$

$$\psi_y(\boldsymbol{r}) = \sqrt{\frac{8}{L_x L_y L_z}} \cos\left(\frac{\pi x}{L_x}\right)\sin\left(\frac{2\pi y}{L_y}\right)\cos\left(\frac{\pi z}{L_z}\right),$$

$$n_2 = 2,\ n_1 = n_3 = 1.$$

The QD is said to be an 'electronic' cavity that localises standing de Broglie waves in space, i.e. electronic wave functions in the conduction band. This QD is located near (in our case, inside) the optical MC, in the spectrum of which there are two almost degenerate photonic modes with frequencies ω_{cx} and ω_{cy} and mutually orthogonal polarisations. Let one of the mechanical modes of the plate have a frequency ω_m close to the frequencies ω_x and ω_y of the electronic transitions in the QD and the frequencies of the optical MC modes. We also assume that the orientation of the QD and MC symmetry axes is such that the $x(y)$ mode of the MC is associated with the optical dipole transition $|g\rangle \leftrightarrow |x(y)\rangle$, and the phonon mode interacts with each of these transitions. Then the Hamiltonian H describing this optoelectromechanical system can be represented as a sum of the Hamiltonian H_0 of isolated subsystems and the interaction Hamiltonian H_{e-c-m}:

$$H_0 = \omega_x |x\rangle\langle x| + \omega_y |y\rangle\langle y| + \omega_{cx} a_x^\dagger a_x + \omega_{cy} a_y^\dagger a_y + \omega_m b^\dagger b, \quad (3)$$

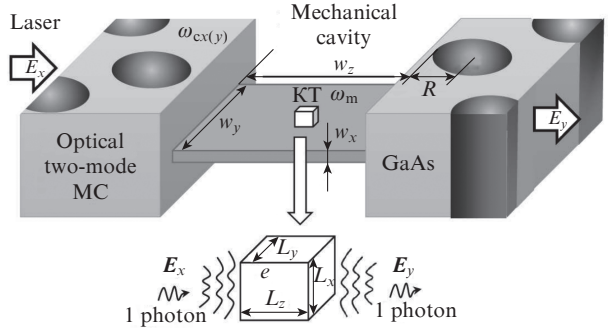

Figure 1. Active region of the polarisation converter representing a single-electron semiconductor QD formed within a thin plate (mechanical resonator), which is attached to a PC-based optical MC (top), and also the converter operation diagram (bottom). After the interaction of a photon with a QD and a mechanical resonator, the polarisation vector of its electromagnetic field $\boldsymbol{E}_x$ changes to $\boldsymbol{E}_y$ (see the text and Fig. 5).

$$H_{e-c-m} = \Omega_{cx} |g\rangle\langle x| a_x^\dagger + \Omega_{cy} |g\rangle\langle y| a_y^\dagger + (\Omega_{mx} |g\rangle\langle x| + \Omega_{my} |g\rangle\langle y|) b^\dagger + \text{h.c.} \quad (4)$$

Here $a_{x(y)}$ and b are the annihilation operators of the excitation quantum in the corresponding mode; and $\Omega_{cx(y)}$ and $\Omega_{mx(y)}$ are the interaction energies of the QD electron and this mode (Rabi frequencies), all frequencies being given in energy units. For continuous supply of electromagnetic energy to the MC, laser radiation is used, which populates the x mode of the MC with photons with frequency ω_L and amplitude $\Omega(t)$, smoothly depending on time. The Hamiltonian H_L makes allowance for this effect:

$$H_L = \Omega(t)(a_x^\dagger + a_x)\cos(\omega_L t/\hbar). \quad (5)$$

The envelope of the amplitude of a laser (tangential) pulse switched on at the time moment t_0 is characterised by the energy Ω_L, duration Δt, and turn-on time τ:

$$\Omega(t) = 0.5\Omega_L\left[\tanh\left(\frac{t - t_0}{\tau}\right) - \tanh\left(\frac{t - t_0 - \Delta t}{\tau}\right)\right]. \quad (6)$$

Finally, we obtain the Hamiltonian

$$H = H_0 + H_{e-c-m} + H_L. \quad (7)$$

We introduce the detuning frequencies of electronic transitions in a QD, of MC modes and of a phonon mode from the laser radiation frequency:

$$\delta_{x(y)} = \omega_{x(y)} - \omega_L,\ \delta_{cx(y)} = \omega_{cx(y)} - \omega_L,\ \delta_m = \omega_m - \omega_L. \quad (8)$$

Then, passing to the reference frame associated with the laser pulse and applying the rotating wave approximation, we can rewrite the Hamiltonians H_0 and H_L as

$$H_0 = \delta_x |x\rangle\langle x| + \delta_y |y\rangle\langle y| + \delta_{cx} a_x^\dagger a_x + \delta_{cy} a_y^\dagger a_y + \delta_m b^\dagger b,\quad H_L = \Omega(t)(a_x^\dagger + a_x). \quad (9)$$

We limit ourselves to the case when the system energy does not exceed the energy of a single optical quantum. Then the dimension of the space of basis vectors of the form $|k, n_x, n_y, n_{phn}\rangle$, where n_{phn} is the number of phonons, $k = g, x, y$, and $n_x + n_y + n_{phn} \leqslant 1$, is equal to 6. The evolution of the system is described by the Lindblad equation for the density matrix ρ:

$$\frac{d\rho}{dt} = -i[H, \rho] + L(\rho). \quad (10)$$

The dissipative effects associated with the uncontrolled escape of photons from the MC at a rate $\kappa_{x(y)}$, photon decay at a rate κ_m, electron relaxation at a rate $\gamma_{rx(y)}$, and dephasing of the QD electronic states at a rate $\gamma_{dephx(y)}$ are taken into account (in the Markov approximation) using the dissipative operator $L(\rho)$ in the Lindblad equation:

$$L(\rho) = \kappa_x D(a_x) + \kappa_y D(a_y) + \kappa_m D(b) + \gamma_{rx} D(|g\rangle\langle x|) + \gamma_{ry} D(|g\rangle\langle y|) + \gamma_{dephx} D(|x\rangle\langle x| - |g\rangle\langle g|) + \gamma_{dephy} D(|y\rangle\langle y| - |g\rangle\langle g|). \quad (11)$$

Here, the expression $D(O) = O\rho O^{\dagger} - [O^{\dagger}O, \rho]/2$ simulates the decay of the value corresponding to the operator O. By solving equation (10) with the corresponding initial conditions, we find the time dependences of the probabilities of populating the hybrid system states. Our task is to select the parameters of Hamiltonian (7) in such a way as to perform a complete or partial conversion of the polarisation of a photon or a weak laser field.

3. Mode structure of optical and mechanical cavities

First, we select the parameters of the optical MC such that its two modes, whose electric and magnetic field projections are mutually orthogonal, have the frequencies $\omega_{cx(y)}$ near the frequencies $\omega_{x(y)}$ of the electronic transitions $|g\rangle \leftrightarrow |x(y)\rangle$ in the QD located in one of the antinodes of the MC electric field. As an MC, we choose a two-dimensional PC, in the centre of which a defective region is located to ensure the electromagnetic field localisation. Modern technologies allow integration of a single QD or their ensembles into a photonic crystal, while auxiliary equipment provides control of the total quantum evolution of electrons and photons in such a hybrid system [9–11]. The PC is a thin GaAs plate with a refractive index of 3.4, in which a periodic triangular lattice of holes is etched (Fig. 1). The defective region where the QD is located is formed due to the absence of one hole in the PC centre (H1 defect). Simulation of the structure's optical spectrum with the lattice constant $a = 11.54$ μm and the aperture radius $R = 0.37a$ using the finite time domain method has shown the presence of two modes in the bandgap of the photonic crystal near a wavelength of 34 μm corresponding to the optical phonon frequency GaAs $\omega_m \approx 0.036$ eV in GaAs. The mode with a wavelength of $\lambda_{c1} = 34$ μm is the so-called TE mode, for which $E_z = H_x = H_y = 0$, and the mode with $\lambda_{c2} = 34.28$ μm is the TM mode ($H_z = E_x = E_y = 0$), which is orthogonal to the TE mode. The two-dimensional distribution of the electric field E of these modes in the plane where the QD is located is shown in Fig. 2. Near the centre of the PC defective region, the electric field amplitude E_0 at the antinode is about 3.5 V cm^{-1} for a plate thickness of 5 μm. Since the QD size in our case is ~17 nm, which is significantly less than the characteristic size of the antinode, the electric field strength can be considered to be constant when calculating the interaction coefficient $\Omega_{cx(y)} = \langle x(y)| - e\boldsymbol{Er}|g\rangle$ (e is the electron charge), and the estimated value $\Omega_{cx(y)} \approx 6 \times 10^{-6}$ eV can be obtained.

As will be shown in Section 4, the most efficient operation of the converter is provided when the mechanical and optical modes converge (resonance); therefore, it is necessary to investigate the possibility of selecting the frequencies of orthogonal optical MC modes. To date, several methods for modifying the MC optical spectrum based on a PC have been developed [9]. This is achieved by exposing the sample surface to an atomic force microscope, applying substances with a refractive index different from that of the PC material, and controlling the temperature using laser radiation or heating microelements embedded into the crystal structure. An equally effective method of spectrum tuning is a small change in the structure of photonic crystal holes near the field localisation region [12–14]. In this work, we replaced the round holes closest to the defective region with elliptical ones and tuned the MC frequencies by adjusting the ellipse eccentricity ε. Figure 3 shows the spectra of the TE and TM modes at various ε. It is seen that with increasing parameter ε, the wavelengths of both

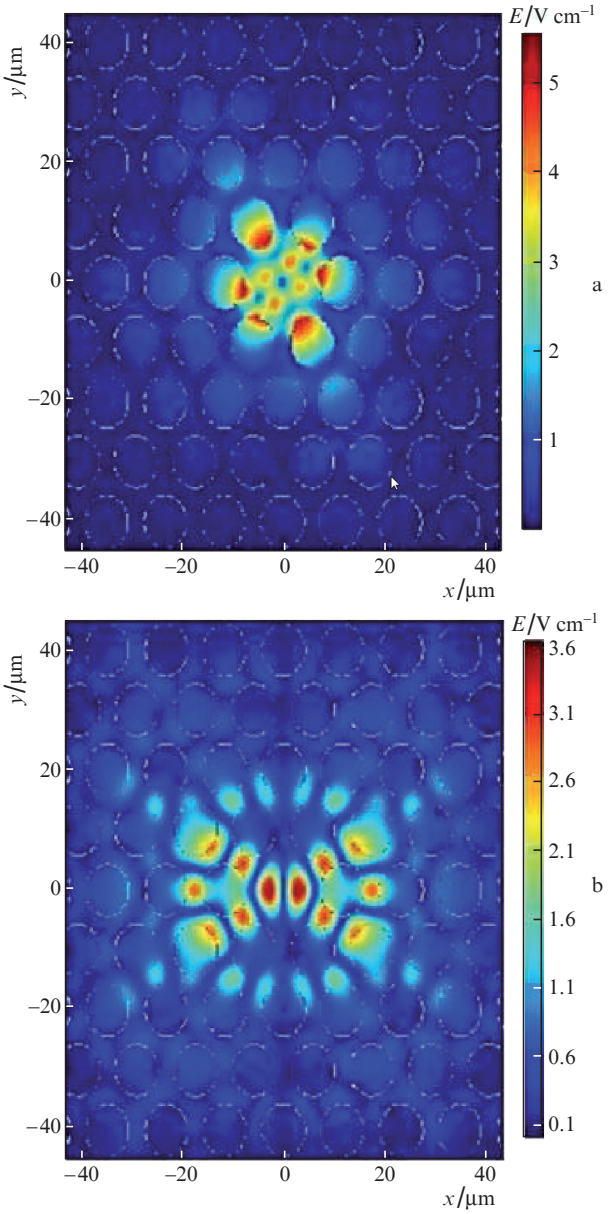

Figure 2. (Colour online) Two-dimensional distribution of the electric field E in a PC for (a) TE and (b) TM modes.

modes grow, and their splitting increases. At $\varepsilon = 0$ (round holes), these modes are degenerate, but a small asymmetry in the hole structure near the PC defect eliminates the degeneration. It is important to note that the electric field amplitude E_0 virtually does not change with changing ε.

To calculate the electron–phonon interaction coefficient $\Omega_{mx(y)}$, we use the approach developed in works [15, 16], where the interaction of a cubic QD and localised optical phonons, whose frequency spectrum is a set of discrete modes, was studied. Such an interaction causes electron transitions between the ground and excited levels of quantum dots. If the mechanical cavity dimensions $w_{x(y,z)}$ are close to that of a QD, $w_{x(y,z)} \approx L_{x(y,z)} \approx 17$ nm, the calculations performed within the framework of this model give $\Omega_{mx(y)} \approx 10^{-3}$ eV, which is several orders of magnitude higher than the value of $\Omega_{cx(y)}$. For the polarisation converter to function, it is necessary that the $\Omega_{mx(y)}$ and $\Omega_{cx(y)}$ coefficients are close (see Section 4); therefore, in this work, the role of the mechanical cavity is

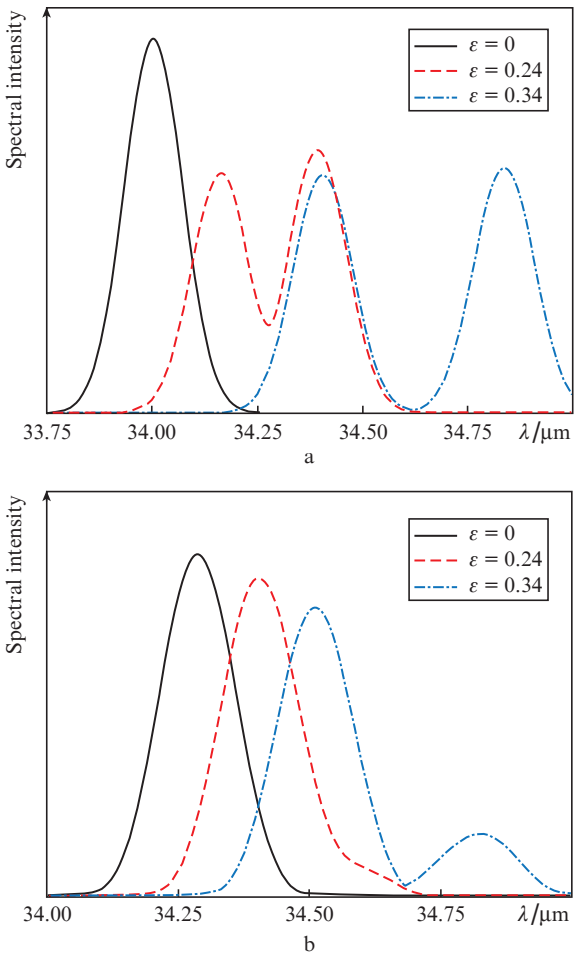

Figure 3. Spectra of (a) TE and (b) TM modes at various parameters of ε.

played by a thin plate with dimensions $w_x \ll w_y, w_z$. The coefficient $\Omega_{mx(y)}$ of electron interaction with a single optical phonon mode with an index $(m_1\, m_2\, m_3)$ in such a plate is expresses as [15, 16]

$$\Omega_{mx(y)} = \sqrt{\frac{16\pi e^2 \omega_m}{q_m^2 w_x w_y w_z}\left(\frac{1}{\varepsilon_\infty} - \frac{1}{\varepsilon_0}\right)(f_m + 1)}\, I_{mx(y)},$$
$$q_m^2 = \pi^2\left(\frac{m_1^2}{w_x^2} + \frac{m_2^2}{w_y^2} + \frac{m_3^2}{w_z^2}\right),\ m_k = 1, 2, 3, \ldots, \qquad (12)$$

where $\varepsilon_0 = 13.2$ and $\varepsilon_\infty = 10.9$ are static and high-frequency GaAs permittivities [17]; f_m is the number of phonons with momentum q_m; and

$$I_{mx(y)} = \int d\boldsymbol{r}\psi_g(\boldsymbol{r})\phi_m(\boldsymbol{r})\psi_{x(y)}(\boldsymbol{r}),$$
$$\phi_m(\boldsymbol{r}) = \sin\frac{\pi m_1}{w_x}\left(x + \frac{w_x}{2}\right)\sin\frac{\pi m_2}{w_y}\left(y + \frac{w_y}{2}\right) \qquad (13)$$
$$\times \sin\frac{\pi m_3}{w_z}\left(z + \frac{w_z}{2}\right)$$

is the dimensionless overlap integral. Since, as was already mentioned, for the converter to operate, it is necessary that the frequencies $\omega_{x(y)}$ are close to the ω_m frequency, the characteristic QD size should be approximately equal to 17 nm. Hereafter, we assume that the optical phonon energy is much greater than the system temperature, $\omega_m \gg k_B T$ (k_B is the Boltzmann constant), and, therefore

$$f_m = \{\exp[\omega_m/(k_B T)] - 1\}^{-1} \ll 1.$$

Calculation of the Ω_{mx} value for lower phonon modes at $w_{y(z)} = 300$ nm and $L_{y(z)} = 17$ nm (Fig. 4) has shown that for large w_x, an increase in the QD size L_x contributes to an increase in the energy of electron interaction with lower phonon modes, while the extreme points in the $\Omega_{mx}(w_x)$ dependences are shifted to the right. By selecting the plate thickness and QD sizes, the coefficient Ω_{mx} can be adjusted. For example, at $w_x \approx 45$ nm and $L_x = 20$ nm, the electron–phonon interaction coefficient Ω_{mx} for the (121) mode is $\sim 6 \times 10^{-6}$ eV, i.e. approximately equal to $\Omega_{cx(y)}$.

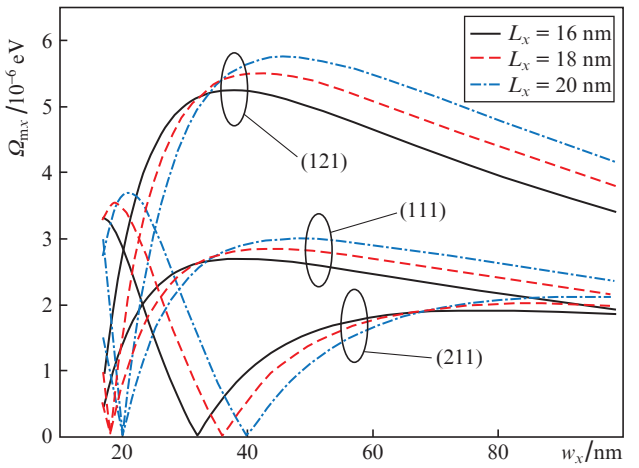

Figure 4. Dependences of the electron–phonon interaction coefficient Ω_{mx} on the plate thickness w_x for the lower phonon modes with indices $(m_1\, m_2\, m_3)$ at $w_{y(z)} = 300$ nm, $L_{y(z)} = 17$ nm and various L_x.

4. Hybrid system dynamics in the coherent regime and manipulations with a single photon

To control the photon polarisation vector, a physical mechanism is needed that implements the effective interaction of the two orthogonal components of this vector. Let us assume that the x mode of the MC is populated by a single photon. How can we convert it to y mode of the MC, i.e. change the polarisation by the angle $\pi/2$? It is known that the addition of an atom-like system to the MC structure modifies its optical properties due to quantum nonlinearity (Purcell effect) [18]; however, the dipole optical transitions responsible for this effect occur with preservation of photon polarisation. In addition, direct transitions between the excited x and y states of an atom are forbidden by selection rules. In work [15], an alternative mechanism for the excitation of electronic transitions in the QD under the action of mechanical deformation (phonons) was proposed. The interaction of the phonon optical mode with the QD electron is described by the Fröhlich Hamiltonian, which does not forbid the energy exchange between modes simultaneously with electronic transitions of different polarisations. Connecting two V-schemes of the transitions between the QD electronic levels, stipulated by the interaction with two MC photon modes and one phonon mode of the plate,

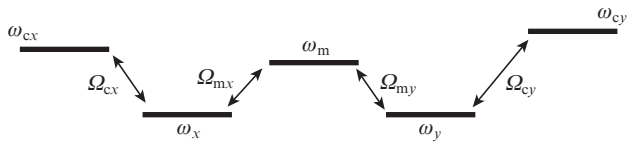

Figure 5. W-scheme of transitions stipulated by the interaction of an electron with two MC photon modes and one phonon mode of the plate, which ensures the rotation of the photon polarisation vector.

we obtain a W-scheme (Fig. 5), which describes the process of rotation of the photon polarisation vector.

To simulate the conversion of single-photon polarisation, we set $\Omega_L = 0$ in Eqn (10) and select the initial condition corresponding to the presence of a QD in the ground state g and an MC with a photon in the x mode. Analysis of population dynamics in atom-like systems indicates the existence of several conditions necessary for the complete transition from one state of the system to another. These conditions in some way or other are related to maintaining the symmetry of transitions. In the simplest case of strict resonance, all Rabi frequencies must coincide to ensure synchronisation of population transfer. Otherwise, beats occur that prevent population of the final state with unit probability (in the absence of dissipation). More complex variants are possible in the tuning regime, when the deviation of one of the parameters (for example, frequency detuning) from its value in the case of a symmetric configuration is compensated by the controlled asymmetry of the other parameter [19].

Figure 6 shows time dependences of the populations of states corresponding to the photon position in MC modes with x and y polarisations. The Hamiltonian parameters are given in effective atomic units for GaAs (Ry_{GaAs} = 6 meV). They correspond to high-Q quantum optical structures in which the energy of the electron–photon interaction reaches 10^{-6}–10^{-5} eV, and the dissipation rates do not exceed 10^{-7} eV. We assume that the transition frequencies in the QD, the MC photon mode frequencies, and the mechanical mode frequency coincide (strict resonance). It can be seen that the

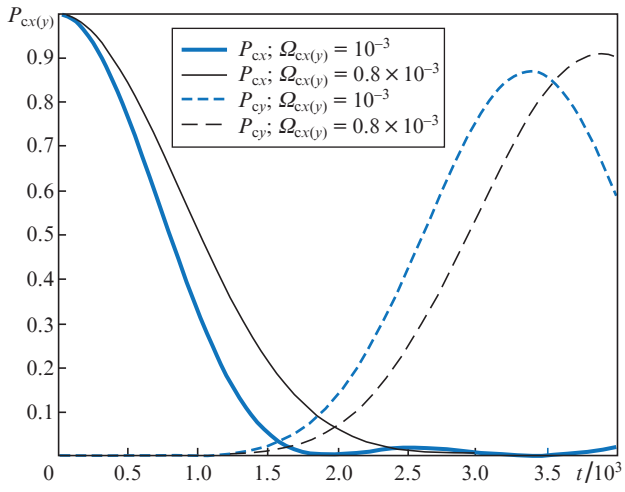

Figure 6. Time dependences of the $P_{cx(y)}$ populations of orthogonal photon modes of the cavity for two values of the energies $\Omega_{cx(y)}$ of the electron--photon interaction at $\Omega_{mx(y)} = 10^{-3}$, $\delta_{cx(y)} = \delta_m = 0$, $\kappa_{x(y)} = \kappa_m = 10^{-5}$, $\gamma_{rx(y)} = \gamma_{dephx(y)} = 10^{-5}$.

photon transition from x mode to y mode occurs during the time $T_{conv} \approx 1/\Omega_{cx(y)}$ with a probability of about 90%. Incomplete transfer is largely due to energy losses associated with dissipative processes. In addition, the probability of transfer depends on the interaction energies of an electron with photon and phonon fields and on the frequency detunings. In particular, the choice of energies $\Omega_{cx(y)} = 0.8\Omega_{mx(y)}$ increases this probability compared to the probability in the case of a fully symmetric configuration: $\Omega_{cx(y)} = \Omega_{mx(y)}$. It can be shown that, provided all relaxation processes are completely suppressed, this choice is optimal and leads to a 100% conversion of the photon polarisation in an MC (Fig. 7). Based on the analysis of the dependence of the maximum probability value P_{cy} (hereinafter, the polarisation conversion probability P_{conv}) on each of the dissipation rates separately, it can be argued that the main contribution is made by the processes of escape of photons from the MC modes to the continuum.

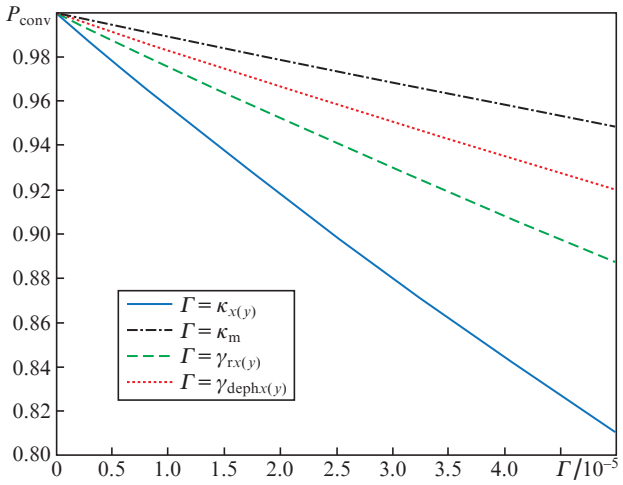

Figure 7. Dependences of the probability P_{conv} of polarisation conversion for each of the relaxation processes separately (i.e., in the complete absence of other decay channels) on the decay rate Γ at $\Omega_{cx(y)} = 0.8 \times 10^{-3}$, $\Omega_{mx(y)} = 10^{-3}$, $\delta_{cx(y)} = \delta_m = 0$.

As we have already noted, the population dynamics described by the W-scheme and implementing the transition from one state to another requires synchronisation of the rates (interaction energies) of all elements of the scheme. On the other hand, due to technological errors, it is impossible to select parameters that strictly comply with this condition. Therefore, it is important to study the issue of the stability of solutions to equation (10) in a certain domain of parameters. The conversion probabilities for independently varying the electron–photon (phonon) interaction energies $\Omega_{c(m)x}$ and $\Omega_{c(m)y}$ and the fixed electron–phonon (photon) interaction energy $\Omega_{m(c)x} = \Omega_{m(c)y}$ are shown in Fig. 8. Analysis of the dependences indicates the existence of several regions along the $\Omega_{c(m)x} = \Omega_{c(m)y}$ line, where the P_{conv} probability reaches 0.9, and the tolerance for parameter deviations (relative to the region size) is 20%–50%. This indicates that the conversion algorithm can be implemented for these regions, even if the parameters deviate significantly from the symmetric case. The most preferred option is to select a region with the parameters specified in the caption to Fig. 8. The ratio $\Omega_{cx(y)}/\Omega_{my(x)} = 0.8$ reflects the dynamic nonequivalence of optical modes, each associated with only

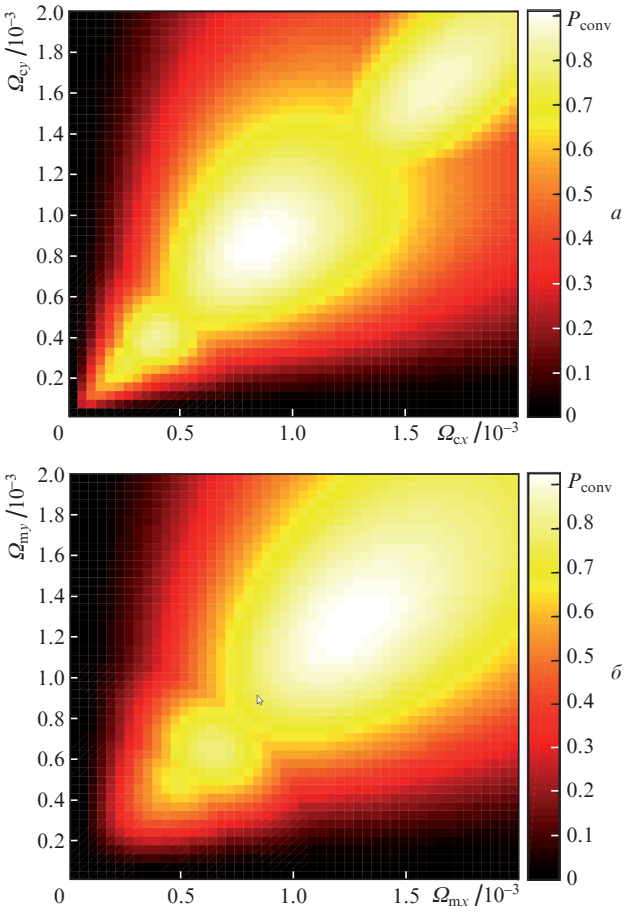

Figure 8. (Colour online) Probabilities P_{conv} of polarisation conversion as functions of sets of independent parameters (a) Ω_{cx}, Ω_{cy} at $\Omega_{mx} = \Omega_{my} = 10^{-3}$ and (b) Ω_{mx}, Ω_{my} at $\Omega_{cx} = \Omega_{cy} = 10^{-3}$ in the resonance regime for $\delta_{cx(y)} = \delta_m = 0$, $\kappa_{x(y)} = \kappa_m = 10^{-5}$, $\gamma_{rx(y)} = \gamma_{dephx(y)} = 10^{-5}$.

one electronic transition, and a mechanical mode that interacts simultaneously with two electronic transitions.

Other parameters that strongly affect the conversion probability are the differences (detunings) between the QD transition frequencies and MC frequencies. It is known that in a three-level system, an increase in detunings from zero to the values that exceed the interaction energy by an order of magnitude, while maintaining a two-photon resonance, is accompanied by a transition from the resonance mode to the Raman mode [18]. In this case, the population of the excited (intermediate) level in a QD does not exceed 1 %, which leads to a significant suppression of relaxation. In our five-level scheme, the phonon mode serves as an intermediate element linking photons with x and y polarisations. Consider the effect of detuning its frequency from the frequencies of optical modes on the conversion probability. Figure 9 shows the dependences of P_{conv} on the detuning δ_m for three values of the electron–phonon interaction energy $\Omega_{mx(y)}$. With small detunings, the P_{conv} value oscillates with a frequency inversely proportional to the energy $\Omega_{mx(y)}$, and then exponentially decays. For the interaction energy $\Omega_{mx(y)} = 2\Omega_{cx(y)}$, in addition to reducing the attenuation caused by the dissipation of the mechanical mode, there is also an increase in the conversion probability to 83% at $\delta_m = 0.007$, compared to 73% at $\delta_m = 0$. Therefore, the Raman mode is also possible in the conditions of hybrid photon–phonon QD control with a sufficiently strong electron–phonon interaction.

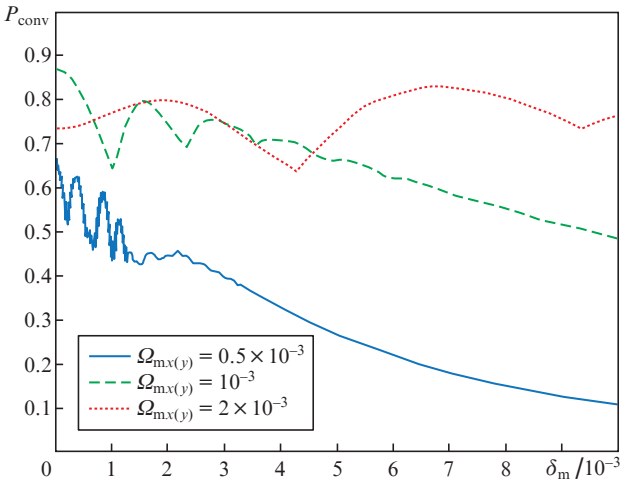

Figure 9. Probability P_{conv} of polarisation conversion as a function of the mechanical mode frequency detuning from the QD and photon mode frequencies, which are considered the same, for three values of the electron--phonon interaction energy at $\Omega_{cx(y)} = 10^{-3}$, $\delta_{cx(y)} = 0$, $\kappa_{x(y)} = \kappa_m = 10^{-5}$, $\gamma_{rx(y)} = \gamma_{dephx(y)} = 10^{-5}$.

5. Polarisation conversion of a weak laser field in steady-state regime

The steady-state regime of propagation of an optical field through a quantum system is usually used to monitor its spectral properties. In addition, maintaining electromagnetic energy in the MC for a long time at a certain constant level, determined by the pulse energy of the control laser and the dissipation rate in the MC [20], may be of particular interest for optically controlled transistor circuits. In this case, switching the field polarisation may be required if the MC modes with orthogonal polarisations control the energy distribution between different subsystems (for example, ensembles of quantum dots or defects), for which the pulse selection rules are essential. In this case, the small (subphoton) field amplitude ensures high sensitivity of measurements of the tested system using transmission spectroscopy and reflectometry methods [8].

Let us select the following parameters of the laser pulse (6) that pumps electromagnetic energy into the x mode of the MC: $\tau = 10^4$, $t_0 = 5 \times 10^4$, $\Delta t = 3 \times 10^5$, and $\Omega_L = 10^{-3}$. If the system was in a vacuum state, this energy would be redistributed between the QD and MC modes. At the initial stage of pulse action, the populations of states oscillate, which indicates a coherent nature of evolution; however, with increasing time, dissipative processes begin to prevail. As a result, the system passes over into a steady state and the populations take stationary values (Fig. 10). After the pulse is turned off, they decrease exponentially to zero. Thus, the calculations confirm the possibility of converting the radiation polarisation also in the steady-state regime. Thus, the calculations confirm the possibility of the radiation polarisation conversion in the steady-state regime. However, unlike the coherent mode, the MC contains both x and y field components. In this case, the average number of photons of the original and transformed fields is approximately the same: $\langle n_x \rangle \approx \langle n_y \rangle \leqslant 0.2$. Since in the MR based on a defect in a two-dimensional PC, the radiation of modes with orthogonal polarisations propagates in different directions, spatial separation of these components can be attained. We emphasise that both components contain informa-

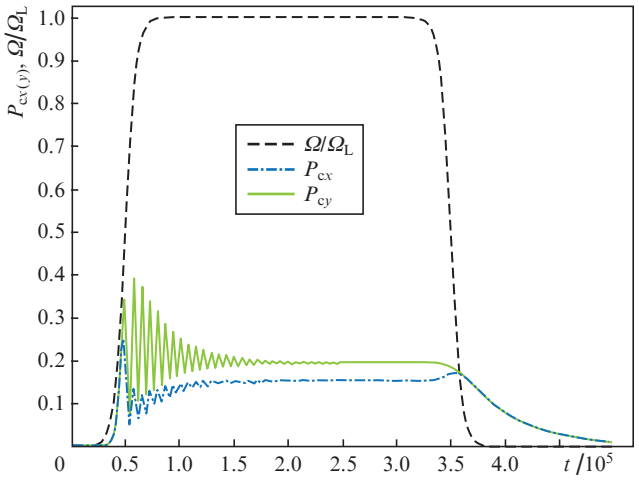

Figure 10. Time dependences of the populations P_{cx} and P_{cy} of the MC photon modes in the case of strict frequency resonance and identical interaction energies under the impact of a laser pulse of tangential shape $\Omega(t)$ (6) for $\Omega_{cx(y)} = \Omega_{mx(y)} = \Omega_L = 10^{-3}$, $\delta_{cx(y)} = \delta_m = 0$, $\kappa_{x(y)} = \kappa_m = 10^{-5}$, $\gamma_{rx(y)} = \gamma_{dephx(y)} = 10^{-5}$.

tion about the internal structure of the QD and the MC. Further use of these stationary incoherent subphoton fields depends on the objectives of the experiment. As a rule, they are used for quantum measurements in transmission spectroscopy and reflectometry.

How will the populations of modes behave when the control pulse energy increases? The answer to this question is given by the dependences shown in Fig. 11. For the interaction energies of laser radiation and x mode, which are close to the interaction energies between the subsystems, close populations of two optical and mechanical modes are also observed in the range 0.15–0.2. As the Ω_L energy increases, the x mode population tends to an equilibrium value of 0.5 (similar to the $|x\rangle$ excited state population in a QD), while the populations of the y mode and mechanical mode decrease to zero. We can speak of a dynamic blockade of the mechanical mode and, as

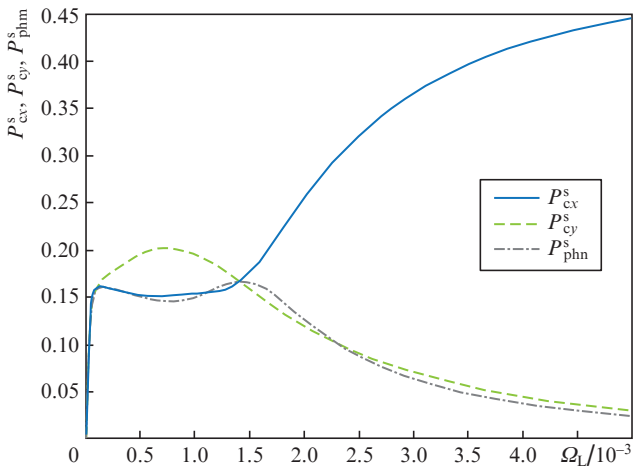

Figure 11. Dependences of the populations P^s_{cx}, P^s_{cy} and P^s_{phn} of the photon and phonon MC modes in the steady-state regime on the energy of laser radiation when it interacts with the MC x mode (strict resonance of all subsystems) for $\Omega_{cx(y)} = \Omega_{mx(y)} = 10^{-3}$, $\delta_{cx(y)} = \delta_m = 0$, $\kappa_{x(y)} = \kappa_m = 10^{-5}$, $\gamma_{rx(y)} = \gamma_{dephx(y)} = 10^{-5}$.

a result, the termination of the energy supply into the y mode. This behaviour of populations is stipulated by the velocity imbalance caused by increasing interaction of the x mode with the transition $|g\rangle \leftrightarrow |x\rangle$ in the QD, while in its absence ($\Omega_{cx} = 0$), a linear increase in the average number of photons $\langle n_x \rangle$ is observed in this mode.

The mechanical mode population as a function of the laser pump energy first reproduces a similar dependence for the x mode, and then, for the y mode. We should add that the practical use of a QD for the generation of electromagnetic radiation was demonstrated in the works of the team led by Zh.I. Alferov, dedicated to semiconductor long-wavelength lasers (see, for example, [21, 22]).

6. Conclusions

Studies on various optomechanical systems, including those based on a semiconductor QD in thin plates, which, thanks to correctly selected geometric parameters, are capable of concentrating single-photon and single-phonon fields, indicate the prospects for using these devices in modern nanoelectronics. The inclusion of a new element – mechanical mode – in the traditional optical design of an MC-based quantum chip, waveguides and lasers, opens up new possibilities for controlling the state of quantum systems that are part of the chip structure. As shown in the present work, the mechanical mode can play the role of an intermediary in the coherent energy exchange between two orthogonal optical modes of the defective PC region of a photonic crystal due to the interaction of phonon and electron in the QD.

This modification of the chip ensures a relaxation of the selection rules, facilitating optical control of the qubit state based on a single-electron QD, generation of stationary subphoton radiation, and polarisation conversion of the initial laser beam. These processes are very important for executing quantum algorithms and reading qubit states. Note that, as in purely optical schemes, for the successful implementation of these operations, it is necessary to properly select the coefficients of interaction and frequency detunings of the subsystems, and also strive to minimise dissipative effects.

Acknowledgements. The investigation was supported by Programme No. 0066-2019-0005 of Ministry of Science and Higher Education of Russia for Valiev Institute of Physics and Technology of the Russian Academy of Sciences.

References

1. Khitrova G., Gibbs H.M., Kira M., Koch S.W., Scherer A. *Nat. Phys.*, **2**, 81 (2006).
2. Michler P. (Ed.) *Single Quantum Dots: Fundamentals, Applications and New Concepts. (Topics in Applied Physics)* (Berlin: Springer, 2003).
3. Blais A., Huang R.S., Wallraff A., Girvin S.M., Schoelkopf R.J. *Phys. Rev. A*, **69**, 062320 (2004).
4. Aharonovich I., Santori C., Fairchild B.A., Orwa J., Ganesan K., Fu K.-M.C., Beausoleil R.G., Greentree A.D., Prawer S. *J. Appl. Phys.*, **106**, 124904 (2009).
5. Kimble H.J. *Nature*, **453**, 1023 (2008).
6. Knill E., Laflamme R., Milburn G.J. *Nature*, **409**, 46 (2001).
7. Johne R., Fiore A. *Phys. Rev. A*, **86**, 063815 (2012).
8. Kim E.D., Majumdar A., Kim H., Petroff P., Vučković J. *Appl. Phys. Lett.*, **97**, 053111 (2010).
9. Tsukanov A.V., Kateev I.Yu. *Mikroelektron.*, **43**, 323 (2014).
10. Tsukanov A.V., Kateev I.Yu. *Mikroelektron.*, **43**, 403 (2014).
11. Tsukanov A.V., Kateev I.Yu. *Mikroelektron.*, **44**, 79 (2015).

12. Vučković J., Yamamoto Y. *Appl. Phys. Lett.*, **82**, 2374 (2003).
13. Hagemeier J., Bonato C., Truong T.-A., Kim H., Beirne G.J., Bakker M., van Exter M.P., Luo Y., Petroff P., Bouwmeester D. *Opt. Express*, **20**, 24714 (2012).
14. Skacel M., Pagliano F., Hoang T., Midolo L., Fattahpoor S., Li L., Linfield E.H., Fiore A. *Phys. Rev. B*, **88**, 035416 (2013).
15. Li X.-Q., Nakayama H., Arakawa Y. *Phys. Rev. B*, **59**, 5069 (1999).
16. Tsukanov A.V., Kateev I.Yu. *Quantum Electron.*, **48**, 641 (2018) [*Kvantovaya Elektron.*, **48**, 641 (2018)].
17. Jacak L., Machnikowski P., Krasnyj J., Zoller P. *Eur. Phys. J. D*, **22**, 319 (2003).
18. Scully M.O., Zubairy M.S. *Quantum Optics* (Cambridge: University Press, 1997).
19. Tsukanov A.V., Openov L.A. *Fiz. Tekh. Poluprovdn.*, **38**, 94 (2004).
20. Majumdar A., Kim E.D., Gong Y., Bajcsy M., Vučković J. *Phys. Rev. B*, **84**, 085309 (2011).
21. Maksimov M.V., Shernyakov Yu.M., Kryzhanovskaya N.V., Gladyshev A.G., Musikhin Yu.G., Ledentsov N.N., Zhukov A.E., Vasil'ev A.P., Kovsh A.R., Mikhrin S.S., Semenova E.S., Maleev N.A., Nikitina E.V., Ustinov V.M., Alferov Zh.I. *Fiz. Tekh. Poluprovodn.*, **38**, 763 (2004).
22. Zhukov A.E., Kovsh A.R., Nikitina E.V., Ustinov V.M., Alferov Zh.I. *Fiz. Tekh. Poluprovodn.*, **41**, 625 (2007).